Adiabatic potential-energy surfaces for oxygen on Al(111)

Y. Yourdshahyan,[1,2] B. Razaznejad,[1] and B. I. Lundqvist[1]
[1]*Department of Applied Physics, Chalmers University of Technology and Göteborg University, SE-412 96 Göteborg, Sweden*
[2]*Department of Chemistry and Laboratory for Research on the Structure of Matter, University of Pennsylvania, Philadelphia, Pennsylvania 19104-6323*

(Received 29 May 2001; revised manuscript received 4 September 2001; published 1 February 2002)

The initial stage of oxidation of aluminum, i.e., adsorption and dissociation of the oxygen molecule, is one of the common model systems for molecule-surface interactions and dynamics. It might seem surprising that there are still some unsettled key dynamics issues. To assess how much can be accounted for in an adiabatic description, an extensive first-principles density-functional-theory study of large pieces of the potential-energy hypersurface (PES) of O_2 on the Al(111) surface is performed. Properties calculated for the free-O_2 molecule, the clean Al(111) surface, and atomic O on the Al(111) surface get values close to measured ones and/or earlier calculated ones, which gives confidence in the method. The calculated PES for O_2/Al(111) shows (i) an entrance-channel energy barrier in *only* one channel having the molecular axis *parallel* to the surface, out of many; (ii) a molecularly chemisorbed state, an "O_2^{2-}" precursor state, in all the considered channels with *nonparallel* molecular axis; (iii) potential for abstraction, i.e., dissociative decay by emission of one neutral O atom; and (iv) both single and close-paired atomically adsorbed O atoms as possible end products. Furthermore, the calculated diffusion barrier ($\approx$0.7 eV) for an O adatom on the surface could rule out the thermal motion of the adsorbed O atoms along the surface at low temperatures. The predicted abstraction channel finds compelling evidence in a recent laser/STM study and resolves a long-standing issue of seemingly huge separations between adsorbed oxygen atoms after dissociation on the Al(111) surface. The predicted metastable molecular state should have great consequences for the dynamics and is stabilized by the very nonequivalent Al-surface field on the oxygen atoms of the nonparallel O_2 molecule. The absence of absolute energy barriers in almost all of the considered adiabatic entrance channels suggests nonadiabatic processes to be required to explain the measured low initial sticking probability and its radical growth with increasing translational energy.

DOI: 10.1103/PhysRevB.65.075416 PACS number(s): 68.43.Mn, 73.20.At, 81.65.Mq, 73.20.Mf

I. INTRODUCTION

Materials and substances in atmospheric contact are exposed to gaseous oxygen. For most metals this results in oxide formation, and the exceptions get a noble status, in, e.g., coins and olympic medals. The oxidation of metal surfaces is a phenomenon of outstanding practical importance. The industrial applications of metal oxides are found in several areas, such as microelectronics, materials science, environmental techniques, and combustion. Oxidation of aluminum is often taken as a model case for metal oxidation. In particular, the initial stage of this process, i.e., adsorption and dissociation of the oxygen molecule, is one of the common model systems for molecule-surface interactions and dynamics. Its actors Al and O_2 have simple but yet versatile electron structures. As a scientific problem it has been picked up and left unsolved many times by prominent scientists. Today, when surface science has reached the level of detailed quantitative comparisons between theory and experiment, it might seem surprising that in such comparisons there are still some unsettled key dynamics issues, highlighted here.

Oxidation of aluminum surfaces is particularly interesting: (i) Aluminum is abundant on earth; (ii) technologically, the oxide film formed on aluminum and aluminum-based alloys in air protects the surface against further oxidation and corrosion, a phenomenon with an early explanation given by Cabrera and Mott;[1] (iii) the simple but yet versatile electronic structure of the aluminum surface makes it a model system for oxidation.

Understanding of the processes involved in the oxidation of aluminum is a long-standing subject of study, attracting large amounts of experimental and theoretical work. However, despite the efforts, the microscopic mechanisms governing the onset, promotion, and termination of aluminum oxidation are largely unknown. The unique oxidation features of the Al(111) surface were first described by Gartland in 1977.[2] Since then there have been many attempts to understand the key steps in the oxidation process, including dissociative adsorption of the O_2 molecule on the surface, migration of the O atom on the surface and into the bulk, and formation of the stoichiometric aluminum oxide (Al_2O_3). These attempts have raised several still controversial issues. The essential features of these investigations could be summarized as follows.

(i) The measured initial thermal dissociative sticking probability is very low, $s_0 \approx 10^{-2}$.[2,3] With increasing translational energy of the incoming oxygen molecule the sticking probability grows successively to a value near unity Fig. 1.[3] One simple explanation of this sticking behavior could have been the existence of an activation barrier of about half an eV for dissociation in the entrance channel. So far, such an explanation has found no theoretical support, however.[4–7] There have been some suggestions that nonadiabatic processes provide the basic explanation of the observed behavior.[8–11] One candidate is harpooning,[12] where the first electron tunneling from Al to O_2, the harpooning electron, starts a dissociation process with many intricate features, such as emission of exoelectrons or surface

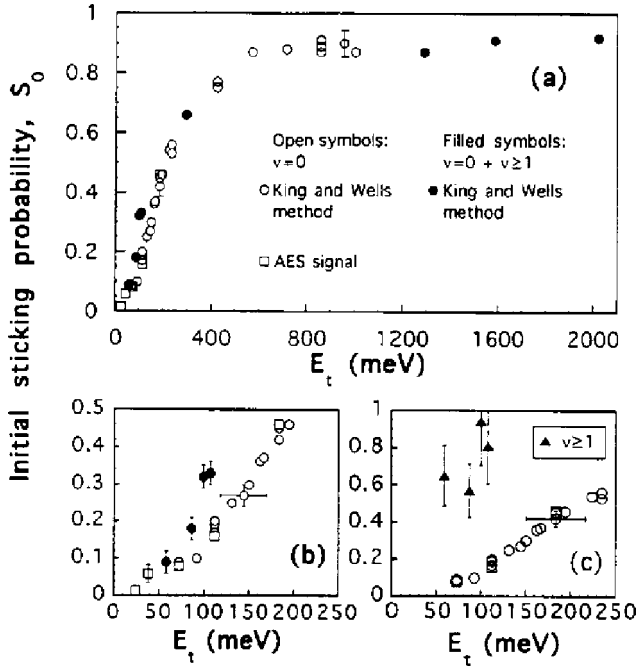

FIG. 1. (a) The initial sticking probability S_0 of O_2 on Al(111), at normal incidence, as a function of translational energy E_t. Open and closed symbols represent experiments with ground-state and mixed ground-state and vibrationally excited O_2 molecules, respectively. The excited-state populations of the latter are as follows (going from low to high E_t): (●) ν=1, 7.5%, 14.7%; 17.5%, 18.9%, 11%, 7.6%, 13.1%, and 17.4%; ν=2, 0.6%, 2.6%, 4.0%, 4.8%, 1.5%, 0.6%, 2.0%, 3.9%, respectively. (b) Enlargment of the low-energy region in (a). (c) Calculated S_0 vs E_t for vibrationally excited molecules (△). Figure is based on Ref. 3.

chemiluminescence.[8] For the harpooning model system, Cl_2 on K,[11,13] such an overlap effect as harpooning occurs relatively far from the surface.[8–11] Since the O_2 molecule has a much lower electron affinity than Cl_2 and the Al surface has a larger work function than K, the first electron transfer from the aluminum surface to the oxygen molecule should occur much more closely to the surface. This makes the O_2/Al(111) system more complicated than Cl_2/K.

Another nonadiabatic possibility is a spin-flip process.[14] The ground state of the free-O_2 molecule is a spin-triplet state with half-filled $2p\pi_g^\star$ molecular-orbital resonance. Chemisorbed oxygen on aluminum is in a fully spin-compensated state, i.e., a spin-singlet state. Thus, the oxygen molecule experiences a triplet-to-singlet spin conversion along the reaction path. The important issues are how effective the triplet-to-singlet transition is and where it occurs. This simple, though appealing, idea as an explanation to the sticking behavior finds no theoretical support, however.[5]

(ii) There exist several contradictory experimental results, which mainly concern the possible existence of a precursor state. Based on separate and independent measurements of the sticking probability and its dependence on the surface temperature, the dissociation of O_2 on Al(111) has been described as both a direct process[3] and one mediated by a molecular precursor.[15] One theoretical study suggests the existence of a molecularly chemisorbed state, an "$O_2{}^{2-}$" state.[7,16] Such a molecular state could be interesting for the dynamics of oxygen adsorption on aluminum surface, a precursor to dissociation expected at elevated temperatures.

(iii) There are also conflicting scanning-tunneling-microscope (STM) results on the fate of the O atoms after dissociation. Results in early STM experiments[17,18] have been given the remarkable interpretation that after the dissociation of a thermal molecule the two O atoms on the Al(111) surface should become separated by at least 80 Å at low coverage. The atoms are also found randomly distributed on the surface, that is, there is no correlation between two neighboring O atoms. The given explanation of this observation is in terms of the so-called "hot-adatom" mechanism.[19] In such a mechanism the energy released during adsorption is transformed to kinetic energy, causing nonthermal motion of the adsorbed O atoms along the surface. Molecular-dynamics simulations based on this idea, using first-principle-calculated data,[20] do not confirm the presence of a large transient mobility of O atoms on the Al(111) surface,[21] as proposed in the STM analysis.

Another proposal[11] is that the dissociation occurs via abstraction,[22] i.e., the emission of one oxygen atom. The idea is that in its approach to the surface at some stage, the O_2 molecule is oriented with its axis perpendicular to the surface or making a small angle to the normal. One of the O atoms should then be absorbed on the surface near the point of impact, while the other atom should be repelled and should fly away from the surface or transfer along it over a large distance. The presence of an O_2^{2-} precursor of this kind has recently been predicted for the O_2/Al(111) system together with a proposal for an abstraction channel.[7,16] Very recently the latter has been corroborated experimentally in a new laser/STM study.[23] At a translational energy of 0.5 eV the dissociative chemisorption of oxygen is documented to give both abstraction of neutral O atoms, uncorrelated atomically adsorbed O atoms, and correlated ones in neighboring fcc sites as end products. The existence of correlated atomically adsorbed O atoms in neighboring fcc sites has also been confirmed in another recent STM study.[24]

(iv) Both experimentally and theoretically, the threefold fcc hollow site is found to be the chemisorption site for O atoms on the Al(111) surface, with a chemisorption energy of about 7.4 eV/atom with respect to the free oxygen atom, with a location of about 0.8 Å from the surface.[20] Nowadays, there is also agreement about the absence of a stable sublayer chemisorption site.[16,25,26]

(v) Another issue to emphasize here is the current stage of theory in predicting properties and resolving problems in surface science. In particular, the density-functional theory (DFT), used here and in numerous other applications with approximate functionals, has an accuracy that cannot be taken for granted. The present generation of implemented functionals still represents approximations to the unknown correct functional. As a matter of fact, the huge inhomogeneity provided by the surface can give unfavorable conditions for their applicability, and it can be argued that surfaces, with their multitude of accurate experimental tools, are important to drive the development of improved functionals.[27] The stated scope of this study is to perform a

state-of-the-art calculation and to see how robust the conclusions are with respect various published density functionals.

The main objective of the present work is to understand and explain the mechanisms involved in the adsorption of an O_2 molecule on the Al(111) surface. The fact that surface science still has unsettled key dynamics issues on the prototype reaction between the O_2 molecule and the Al(111) surface is of course disturbing. To assess how much can be accounted for in an adiabatic description, an extensive state-of-the-art first-principles calculations based on the DFT (Ref. 28) is performed here on the system, and large pieces of the multidimensional potential-energy hypersurface (PES) of O_2 on Al(111) are mapped out together with electron densities of state (parts of these results are already published in Refs. 7 and 16).

The picture that emerges for oxygen adsorption on this surface is an intricate and complex one. For an oxygen molecule approaching an Al(111) surface adiabatically to finally end up as one or two fully chemisorbed O atoms on the surface, there are a great variety of energy landscapes. There are expected features, e.g., charge transfer, and novel ones, such as a pronounced orientational dependence, which open up possibilities for molecular precursors and abstraction. When the molecule has an inclination to the surface plane (*nonparallel* case), i.e., for a large part of phase space, there is a great probability for an intermediate molecularly chemisorbed state. The most stable adsorbed molecular state of such a kind is found in the fcc site, with the molecular axis nonparallel to the surface, with a chemisorption energy of 1.8 eV, and with an electron configuration identified as that of "O_2^{2-}." Such a metastable state for an inclined molecule is argued to be a consequence of the strong variation of the electronic potential in the Al-surface region, from the inner-potential value to the vacuum level. The incentive for spin polarization is accordingly a mechanism completely different from the *d*-electron-dependent one, e.g., O_2 on Pt. A barrier is found only for one of the many studied configurations and locations, with the O_2 molecule having $\phi=\theta=90°$ (variables as in Fig. 5) and center of mass (CM) above a bridge site (Fig. 6, "gray molecule"). Further, the absence of absolute energy barriers in the majority of the entrance channels for O_2 *parallel* to the surface[5,6] (*parallel* case) is confirmed and shown to apply also in all other studied *nonparallel* cases. Our study also identifies uncorrelated atomically adsorbed O atoms and correlated ones in neighboring fcc sites as end products. These O atoms are chemisorbed at the threefold fcc site at a distance of 0.74 Å above the surface and at a chemisorption energy of 7.375 eV/atom with respect to the free-oxygen atom. In the framework of the harmonic approximation the vibrational frequencies for the adsorbed O atom have been calculated to be 50 meV and 54 meV for the perpendicular and the parallel vibrations, respectively. Several calculations aiming at taking into account the nonadiabatic triplet-to-singlet-spin conversion mechanism have been performed, which cannot explain the sticking behavior in a simple way, however. The present study points at an intricate dynamics and an interesting kinetics of oxygen on the (111) surface of aluminum.

The paper is organized as follows. In Sec. II our method of calculation is outlined. In Sec. III we present our results for different parts of our investigation, including the free-oxygen molecule, free-Al surface, single oxygen adsorption, and dissociation of oxygen molecule. Section IV is a discussion of the presented results. Finally, Sec. V provides our major conclusions and outlook.

II. THE CALCULATION METHOD

The calculations presented in this paper are based on the DFT and performed by means of the plane-wave-pseudopotential code DACAPO (massively parallelized over both *k* points and bands).[29] For the exchange-correlation (XC) energy-density functional the generalized-gradient approximation[30–33,29] (GGA) is used. The wave functions are expanded in a plane-wave basis set, and pseudopotentials are used to describe the electron-ion interactions. The Kohn-Sham equations are solved by using the density-mix scheme,[34] in which a Pulay-mixing algorithm is used to update the electronic density between iterations. The occupation numbers are updated using a recently developed technique based on minimization of the free-energy functional. To reduce the number of *k* points needed, a finite electronic temperature of 0.1 eV is used. All total energies are then extrapolated to zero electronic temperature. Vanderbilt's ultrasoft pseudopotentials[35] are used for both O and Al in order to keep the number of plane waves small and thus the calculations less time consuming. All calculations are performed allowing for spin polarization.

The PW91 functional is used as the basic exchange-correlation functional in all the calculations. However, it has been reported[29] that some physical quantities, e.g., the chemisorption energy, depend rather strongly on the choice of the exchange-correlation functional when the density variations are substantial. Therefore, the effects of the new functionals [Perdew-Burke-Ernzerhof (PBE), and revised PBE functionals (revPBE) and RPBE)], (Refs. 32,33 and 29) are investigated by performing calculations with these new functionals and comparing the results with that of the Perdew-Wang-91 (PW91) functional.

When using the slab geometry in the plane-wave-pseudopotential method, errors most often arise from the pseudopotential or from lack of convergence with respect to the number of *k* points, the cutoff energy, and the system size. Therefore, all these issues are taken to account in order to achieve high-quality results.

When generating pseudopotentials it is important to preserve the eigenvalues for all relevant atomic configurations, not just in the reference configuration. However, in order to have correct lattice constants for metals it is also important to preserve the charge density in the tail region for all relevant atomic configurations. We generate new ultrasoft pseudopotentials for all elements involved, with maximum transferability errors less than 2 mRy. All potentials are tested and compared to experiment and to all-electron calculation, showing excellent agreement. For *k* points and cutoff energy convergence, tests are performed using cutoff energies of 20–35 Ry with 2–55 irreducible Monkhorst and Pack (MP) *k* points samplings.[36] A minimum cutoff energy of 25

TABLE I. The equilibrium bond length ($d_{O\text{-}O}$) and binding energies E_b for a free-oxygen molecule using different pseudopotentials for oxygen. Pseudopotentials are generated using PBE functional with (PP-*C*) and without (PP-NC) including the partial core (for details see Ref. 32).

	E_b (eV) [$d_{O\text{-}O}$ (Å)]			
Pseudopotential	PW91	PBE	revPBE	RPBE
PP-NC	5.73 [a] (1.24 [a])	5.95 (1.23)	5.59 (1.23)	5.55 (1.23)
PP-*C*	6.09	6.01	5.65	5.62
PP-*C* (Ref. 32)	6.06 [a]	5.99 [a]	5.63 [a]	5.59 [a]

[a]Values are from an oxygen pseudopotential generated using PW91 functional.

Ry with six irreducible *k* points sampling shows converged results with errors in meV regime.

In order to reduce calculation errors due to finite slab thickness, different slab geometries are tested using different numbers of *k* points and vacuum layers, see Sec. III B for more details. Based on this test results, a slab geometry of six Al and five vacuum layers is chosen. The oxygen molecules are adsorbed on one side of the slab only. The artificial electric field due to the asymmetry of the system is compensated for by means of a correction formula.[37]

In order to optimize the structural parameters and the atomic positions, two different relaxation procedures are used, a damped molecular-dynamics (DMD) method and a hyperplane adaptive constraint method. In the former method, at each step, only the part of the ion displacement velocity that is parallel to the forces of the ion is kept. The latter method is a simplified version of the more general nudged elastic band method of Mills *et al.*[38]

To obtain the PESs, total energies are calculated for different intramolecular distances $d_{O\text{-}O}$ and different CM distances *Z* from the Al surface, with a step size of 0.2 Å and 0.5 Å, respectively. For a smoother PES, a bicubic interpolation algorithm is used, taking into account the forces on the oxygen molecule and energies at each point. Effects of surfaces relaxation are investigated in a few key cases.

III. RESULTS

A. Free O_2 molecule

According to experiment, the equilibrium bond length and the binding energy for a free-oxygen molecule are 1.24 Å and 5.11 eV, respectively. Our calculated DFT-GGA values for the bond length and binding energy for a free-oxygen molecule using different pseudopotentials and exchange-correlation functionals are given in Table I. The agreement between the experimental and calculated results is excellent for the bond length, while the binding-energy value reflects the difficulties of GGA for atomic oxygen (the all-electron value is 6.20 eV). The results obtained by means of the PW91 functional differs from those using other functionals. This is explained by the fact that the pseudopotential has been generated using the PW91 functional.

For later reference, the energy levels of the valence orbitals of the free-O_2 molecule are calculated (Fig. 2). The diagram clearly illustrates the versatility of O_2. There are not only σ and π orbitals and bonding and antibonding orbitals but also a significant spin splitting of the levels. The significance of Hund's first rule is manifested by having the antibonding spin-up π orbitals occupied and the spin-down ones empty reflecting the fact that the O_2 molecule in its ground state is a spin triplet ($S=1$). The $2s$ derived σ_s orbital exhibits a substantial bonding-antibonding separation (about 13 eV) and a noticeable spin splitting of both the bonding and antibonding levels (about 2 eV), and some sp hybridization. A similar situation applies for the $2p_z$-derived σ_p orbital, leaving the antibonding one unoccupied. For the π_p orbitals the bonding-antibonding shift is smaller (about 7 eV), while the spin splitting is about the same (about 2 eV).

B. Clean Al(111) surface

The first step towards an investigation of the aluminum surface is to test the generated pesudopotential with PW91 on bulk aluminum and calculate the structural parameters. The achieved values for the lattice constant ($a=4.04$ Å), the bulk modulus ($B=72.5$ MPa), and the cohesive energy ($E_{coh}=3.5$ eV) compare well with those calculated with other similar methods and those from experiments (Table II).

For the surface calculation, when using slab geometry it is important to reduce errors due to the quantum-size effect,[48] which gives a dependence of the results on the number of Al layers. Therefore, different slab geometries (four, six, and eight layers thick) are tested, where in all cases the two low-

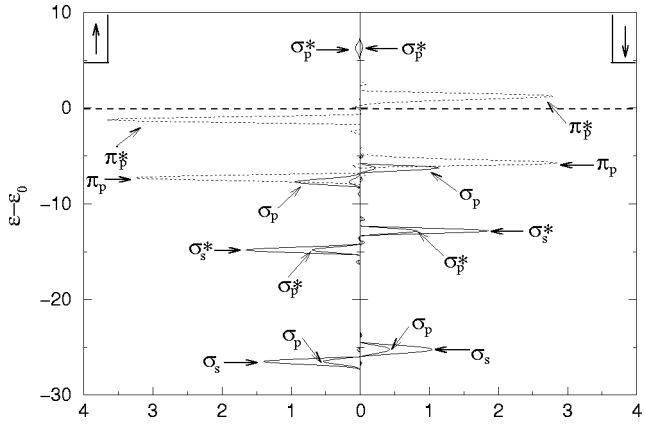

FIG. 2. Energy levels of the valence orbitals of the free-O_2 molecule calculated with the present method. The density of states (DOS) is projected into molecular orbitals. The left and right panels show the spin-up and -down LDOS, respectively.

TABLE II. Calculated bulk properties for Al and comparison with other recent calculations and experiments. PWPP, plane-wave pseudopotential.

Method/XC	a (Å)	$B_{\bigcirc}$ (GPa)	E_{coh}	Ref.
PWPP/LDA	3.971	81.4	4.09	53
	3.970	82.0	4.05	56
LAPW/LDA	3.978	83.9		57
PWPP/PW91	4.040	72.5	3.50	16
	4.039	71.9	3.54	53
	4.030	72.0	3.51	39
LAPW/PW91	4.094	72.6		57
PWPP/PBE	4.050	77.0	3.51	56
	4.045	78.1	3.38	16
Experiment	4.048	77.3	3.39	40
	4.030	79.4,82.0	3.39	41–45

est layers have fixed bulk positions and the remaining layers are only relaxed in the z direction (perpendicular to the surface). The calculations for all these surfaces are carried out using a $4\times4\times1$ MP grid[36] of special k points. The calculated results clearly demonstrate the effect of k points, cutoff energy, and number of layers included in the slab geometry on the results for the Al(111) surface (Tables III and IV).

The surface energy is obtained as

$$\sigma=(1/2)[E_{\mathrm{slab}}(n)-nE_{\mathrm{bulk}}], \tag{1}$$

where $E_{\mathrm{slab}}(n)$ is the total supercell energy for a slab with n Al layers and E_{bulk} is the total bulk energy of one Al layer obtained as

TABLE III. Comparison of calculated results for the interlayer relaxations Δd_{12}, Δd_{23}, and Δd_{34} (1=outermost layer) of the Al surface in different slab geometries [(2×2) surface overlayer]. Note that the super cells consist of "m" Al layers and "l" vacuum layers, respectively. The number of irreducible k points are denoted n_{kp}. The experimental values are marked expt. and the exchange-correlation approximation used in the calculations is marked with LDA and GGA, respectively. The presented results in boldface are the results from a total relaxed slab. For more details see the text.

	n_{kp}	$m+l$	Δd_{12} (%)	Δd_{23} (%)	Δd_{34} (%)
Al(111)					
This work	6	4 + 4	1.00	−0.95	0.40
(GGA)	6	6 + 5	1.15	−0.06	0.18
	6	8 + 6	1.18	−0.21	0.09
	20	**6 + 5**	**1.08**	**−0.10**	**0.05**
Ref. 28 (LDA)		5	1.00	2.00	
Ref. 50 (LDA)	36	9 + 6	0.80	0.50	
Ref. 47 (GGA)			1.00	−0.07	
Ref. 58 (LDA)	2	4	1.38	−2.14	1.08
Ref. 59 (GGA)			1.40		
Ref. 49 (LDA)	37	12	1.18	−0.40	0.22
Ref. 50 (expt.)			1.7±0.3	0.5±0.7	
Ref. 51 (expt.)			0.9±0.5		

TABLE IV. The calculated work-function values for the three optimized low-indexed aluminum surfaces, compared to other theoretical and experimental results. The umarked values are GGA values. In the parentheses the unrelaxed values are given.

	Al(111)	Al(110)	Al(100)
This work	4.18 (4.10)	4.23 (4.17)	4.29 (4.25)
[a] Reference 55	4.25 (4.23)	4.30 (4.29)	4.38 (4.42)
[a] Reference 49	4.31	4.32	4.51
[b] Reference 52	4.24±0.03	4.28±0.02	4.41±0.02

[a]LDA values.
[b]Experimental values.

$$E_{\mathrm{bulk}}=E_{\mathrm{slab}}(n)-E_{\mathrm{slab}}(n-1). \tag{2}$$

The calculated surface energy σ values from Eq. (1) calculated for an increasing number of layers n show convergence only when the of bulk-energy value from Eq. (2) is converged. This confirms the results of Boettger, who also gives more detailed information.[48] Our calculated surface-energy value shows a converged value for a minimum of six Al layers in the slab, $\sigma=0.808$ J/m^2 is in excellent agreement with 0.82 J/m^2 and 0.81 J/m^2 from a similar calculation (using the PW91 functional[56]) and experiment,[57] respectively.

Based on these tests, periodic slabs consisting of six Al and five vacuum layers are chosen (four Al atoms in each layer). Further relaxations are carried out (three outermost layers are fully relaxed, the fourth layer is only relaxed in the z direction, and the remaining layers are kept fixed in bulk positions) using a $8\times8\times1$ MP grid with 25 Ry cutoff energy, and the supercells are totally optimized, until a force-free situation is achieved (sum of the absolute values of the forces is less than 0.05 eV/Å). The calculated values for Δd_{ij} (boldface in Table III) compare reasonably well with those of other calculations and with experimental data. The small outward relaxation for the Al(111) surface reported from experiments is also successfully reproduced.

The calculated work-function values for clean Al(111), Al(100), and Al(110) surfaces (Table IV) confirm the findings of Fall *et al.*[58] regarding the anisotropy of the aluminum work function: For most fcc metals (such as Ni, Cu, and Ag) the values of the work function follow an increasing trend that can be described as (110)→(100)→(111), observed experimentally and predicted by Smoluchowski's rule.[59] On the other hand, for aluminum the experimental and theoretical trend is (111)→(110)→(100). This aluminum work-function anomaly is due to the increased p-atomic-like character of the density of states at the Fermi energy, as compared to most other fcc metals.[58,59]

C. Single-O-atom adsorption on Al(111) surface

Key issues for adatom adsorption are chemisorption site and energy. Generally speaking, there is agreement in the literature about these properties of an oxygen atom on the Al(111) surface. For instance, a recent DFT calculation[25] has shown the O chemisorption site on Al(111) to be in the three-fold coordinated fcc position, the distance from the surface

TABLE V. Calculated adsorption energies of atomic oxygen on Al(111) surface. The adsorption energies [ΔE (eV)] are given in reference to chemisorption energy in the fcc site, the calculated values are for a totally optimized system. The n_{kp} and E_c values denote the number of irreducible k points and the cutoff energy (Ry), respectively. In the parentheses the equilibrium distance [Z (Å)] over the surface is shown.

	ΔE (eV) PW91		RPBE
Site	n_{kp}/E_c 6/25	30/30 (Z)	30/30 (Z)
Fcc	0.000	0.000 (0.74)	0.000 (0.74)
Bridge	0.734	0.716 (0.92)	0.718 (0.92)
Hcp	0.441	0.424 (0.75)	0.425 (0.75)

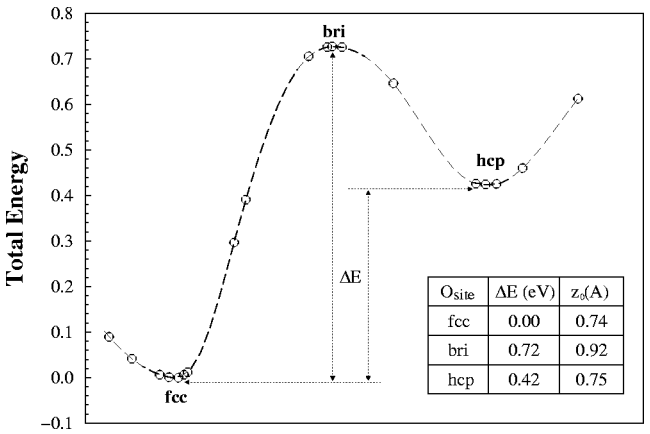

FIG. 3. The total-energy difference for an oxygen atom at several points along the diffusing path shown in Fig. 2. The insetted table shows the relative binding energies and the equilibrium positions over the relaxed first Al layer. In the calculations the Al ions in the three outermost layers are allowed to totally relax.

layer to be 0.86 Å, and the energy to be 5.0 eV/atom with respect to the free-oxygen molecule, which means a chemisorption energy of 7.55 eV/atom ($E_b=5.11$ eV) with respect to the free-oxygen atom. This is a very strong chemisorption bond. These results have been calculated within the local-density approximation (LDA) and using GGA non-self-consistently for the total energy (so-called post-GGA).

The aim of this part of our study is to find out whether improved methods change the picture of single oxygen chemisorption on Al(111) surface, to calculate the PES for an oxygen atom approaching the bare Al surface, and to test our method and generated potentials on a well-known system.

The calculations are performed using a fully optimized slab consistent of six (2×2) Al(111) layers and five layers of vacuum. A single oxygen atom is adsorbed in high-symmetry points of the surface and the whole system is relaxed until total forces are less then 0.1 eV/Å . The effect of k points and cutoff energy are also examined, and converged results are achieved already with $E_{cut}=30$ Ry (Table V). However, in order to reduce the numerical errors to less than 10 meV, a 30 k-point MP sampling and a cutoff energy of 30 Ry are used in all the calculations. Furthermore, the dependence of the chemisorption energy on the coverage is tested, the calculation for a (3×3) Al(111) supercell, i.e., $\Theta=0.11$, producing a change in chemisorption energy by only 18 meV.

The chemisorption energy (per oxygen atom) is defined to be

$$E_{chem}=E_{\mathrm{Al}}+E_{\mathrm{O}}-E_{tot}, \tag{3}$$

where E_{O} is the energy for an isolated oxygen atom in the same supercell and E_{Al} is the energy for a clean Al(111) surface, calculated for an optimized slab by using the same number of sampling k points and the same cutoff energy. In the low-coverage limit ($\Theta=0.25$ in our case) it is calculated in GGA to be $E_{chem}=7.375$ eV/atom, corresponding to 4.527 eV/atom with respect to the free-O_2 molecule (the free-molecule atomization energy is calculated to be $E_b=2.848$ eV/atom). The value is in good agreement with other calculated results, 5.0 eV (Ref. 25) and 4.3 eV (Ref. 5) using post-GGA and GGA, respectively.

The PES along the diffusion path within the surface-lattice unit cell is shown in Fig. 3. Obviously the O atom has the lowest potential energy in the fcc hollow site at a distance of $z=0.74$ Å from the relaxed Al-atom surface layer, in agreement with other studies.[25] The diffusion barrier for a chemisorbed oxygen atom initially in the fcc site is calculated to be 0.72 eV (difference in binding energy for oxygen in fully relaxed fcc and bridge positions, respectively). This value is compared to the recently reported STM result of 1.0–1.1 eV (Ref. 60) and the recent DFT-GGA result of 0.9 eV.[5] The STM value is measured in the temperature range 350–530 K and described by the authors to be in the 10–20 % range of the adsorption energy, which could explain why it differs from our calculated values. Unfortunately, there are very little details of the DFT-GGA calculated values.[5]

The calculation of surface relaxation shows that, when moving the oxygen atom from the fcc site over the bridge into the hcp site, the surface atoms reconstruct in order to lower the total energy. The decrease in energy caused by surface reconstruction is estimated to be 10 meV, 14 meV, and 56 meV for the fcc, hcp, and bridge sites, respectively, showing the great importance of surface relaxation. The detailed results from the study of surface buckling and other surface features of oxygen adsorbed on fcc, bridge, and hcp sites are shown in Fig. 4 and Table VI.

The change in the work function with the O atom in this stable position is calculated to be $\Delta\Phi=0.065$ eV, which can be compared with the clean-Al(111)-surface calculated value of $\Phi=4.18$ eV.

The vibrational frequencies of the oxygen atom are calculated by making small changes in the oxygen position (a few percent of an angstrom), while keeping the Al atoms fixed. In the harmonic approximation they are estimated to be $\hbar\omega_{\perp}=50$ meV and $\hbar\omega_{\parallel}=54$ meV, perpendicular and parallel to the diffusion path, respectively. At the bridge site the result using the same approximation is $\hbar\omega_{\perp}=52$ meV. This method is approximate, but it has been successfully used for determination of vibrational frequencies for O/Pt(111).[61] Fixing the Al surface atoms means that they are assumed to have infinite mass. Naturally, this is not the best assumption, but on the other hand allowing surface relaxation would cause

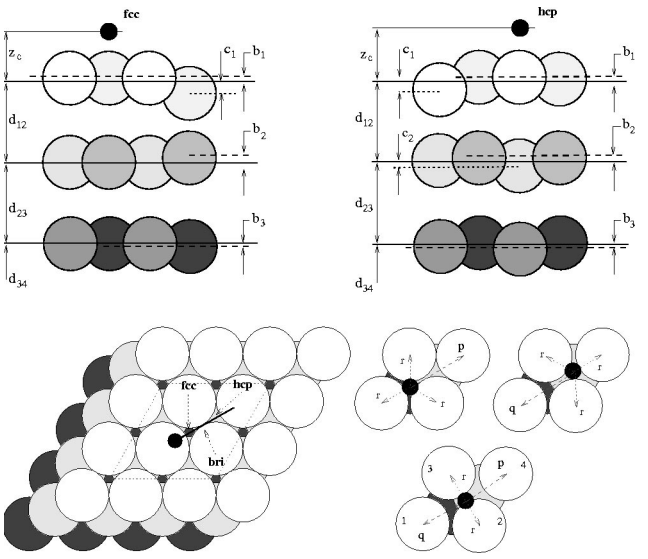

FIG. 4. Schematic presentation of the surface relaxation for the O/Al(111) system with the oxygen atom adsorbed in fcc, bridge (bri), and hcp sites, respectively. The interlayer spacings d_{ij} are measured between center-of-mass planes (solid lines). The bucklings are given by b_i and c_i (dashed lines). The radial displacements of the Al-surface atoms seen from oxygen are shown as r, p, and q. The in-plane rotations of surface atoms compared to the ideal ones are $\Delta\alpha_{1-4}$, where the indexes 1–4 pointing to atoms are shown and marked in lower right figure. The lower left figure shows the bottleneck diffusion path (see Fig. 3 for the barrier) of an oxygen atom on the Al(111) surface. The relaxation effects are summarized in Table VI.

TABLE VI. Calculated surface relaxation for a single O atom on Al(111). The parameters $d_{i,j}$ denote the distance between the center of mass of layers (CML) i and j. The Z_c value shows the distance between the chemisorbed oxygen and the CM of topmost Al layer. The parameters b_i and c_i indicate the buckling in the layer with respect to the CML, where the index i denotes the layer, the r, p, and q denote radial displacements seen from oxygen (Fig. 4), and $\Delta\alpha_i$ denotes the in-plane rotation of nearest neighbors for oxygen atom.

	Fcc (calc.)	Bridge	Hcp
z_c	0.74	0.92	0.75
d_{12}	2.39	2.40	2.39
d_{23}	2.30	2.26	2.27
d_{34}	2.28	2.28	2.27
b_1	0.04	0.07	0.03
b_2	0.01	0.00	0.01
b_3	0.00	0.00	0.00
c_1	−0.09	−0.07	−0.12
c_2	−0.03	0.00	−0.10
$r_{\text{Al-O}}$	1.86	1.76	1.87
p (q)	3.23	2.83(2.78)	3.23
$\Delta\alpha_1=\Delta\alpha_4$	0.00	0.00	0.00
$\Delta\alpha_2=-\Delta\alpha_3$	−0.04	−1.92	0.02
$\Delta\Phi$	0.05	0.06	−0.41

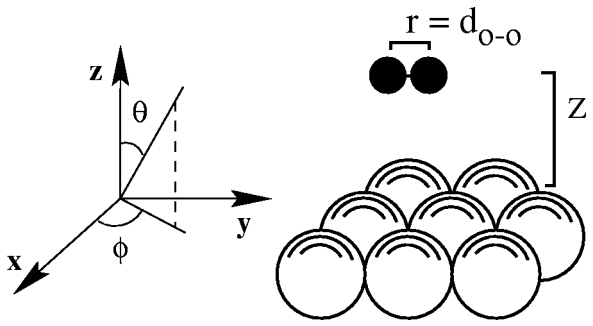

FIG. 5. Schematic figures for molecular orientation on an Al(111) surface. Z, $d_{\text{O-O}}$, θ, and ϕ represent distance from surface plane.

even worse problems. A correction has been suggested by Head,[62] which could be an alternative in solving the problem.

The diffusion prefactor is then determined to be $D_0 \simeq 2.7 \times 10^{-3}$ cm^2 s^{-1}, using $D_0 = 3(l^2\nu_0)/4$, where l is jump length and ν_0 is the so-called attempt frequency or prefactor, which is roughly equal to the vibrational frequency of an adatom. The experimental diffusion-prefactor value is estimated to be 5.0×10^{-3} cm^2 s^{-1}.

D. Van der Waals interaction

At large separations between the O_2 molecule and the Al(111) surface there is only the weak but long-ranged van der Waals interaction. This attraction is responsible for a number of phenomena, e.g., physisorption between an adparticle and a solid surface. Since the motion of the thermal oxygen molecules far outside the aluminum surface could be decisive for the dissociation process the effect of the van der Waals interaction should be included.

The asymptotic form of the van der Waals interaction potential for an atom or molecule outside the surface is[63]

$$E_{vdW}(Z) = -\frac{C_3^{(0)}}{(Z-Z_o)^3}, \tag{4}$$

where Z is the distance between the molecular CM and the Al(111) surface. The coordinates (Z, θ, ϕ, and r) are defined in Fig. 5, C_3^0 is the van der Waals coefficient, and Z_0 is the van der Waals reference-plane position.

Any anisotropy in the interaction is also of interest for the dynamics of thermal oxygen molecules on the Al(111) surface. This effect can cause the impinging molecules to be aligned in a specific orientation with great importance for molecular trapping or abstraction, i.e., give a steering effect. For a homonuclear molecule outside a surface, the van der Waals energy can be expressed as[64,65]

$$E_{vdW}(Z,\theta) = -\frac{1}{(Z-Z_o)^3}[C_3^{(0)} + C_3^{(2)}P_2(\cos\theta)], \tag{5}$$

where θ is the angle between the surface normal and the molecular axis (Fig. 5).

To be able to calculate the van der Waals energy in a DFT framework, one should go beyond the existing LDA and GGA approximations. This is not a failure of DFT itself, but a failure of these approximations due to their local or semilocal nature.[66] Any van der Waals density functional has to be an improved approximation for the exchange-correlation energy that accounts for the truly nonlocal dependencies. Recently a new approximate van der Waals density functional has been proposed,[67,64] from which the van der Waals energy can be calculated within DFT.

According to this theory the van der Waals coefficient C_3^0, the van der Waals reference-plane position Z_0, and the parameter $C_3^{(2)}$ are calculated to be $C_3^{(0)}=1.47$ eV Å^2, $Z_0=0.29$ Å, and $C_3^{(2)}=0.145$ eV Å-^{2}.[68] This makes the van der Waals energy $-1.39/(Z-0.29)^3$ eV for a molecule parallel to the surface and $-1.61/(Z-0.29)^3$ eV for one perpendicular to it. Specifically, at $Z=3.5$ Å, where the van der Waals energy is the dominant source of interaction, this energy is -42 meV and -49 meV for O_2 parallel and perpendicular to the surface, respectively. There is thus a slight anisotropy, with a size that is comparable to thermal energies and energies calculated here with GGA. This could influence the dynamics of thermal O_2.

E. Adiabatic potential-energy surfaces

To describe the dynamics of the oxygen molecule close to the aluminum surface the PES is needed. Although there have been some suggestions[8–10] that nonadiabatic processes are important in the dissociative process of the O_2 molecule, the adiabatic PES is always needed, at least as a reference. Further, the oxygen motion might be on the adiabatic PES. For these reasons we have performed careful and accurate calculations of large pieces of the multidimensional PES of O_2 on Al(111).

Since there might exist different complex trajectories for an O_2 molecule approaching the surface, the work of mapping the PES should be done in a systematic way. For this reason and in order to assess the method by comparing with some available results of other calculations, we first scan the surface and calculate total energies for several different orientations and locations of the O_2 molecule, starting with the CM distance $Z=3.5$ Å above the Al(2×2) surface layer. The distance between the two O atoms is kept at the free-molecule value $d_{O\text{-}O}=1.24$ Å. Calculations are performed for $\theta=0°$, 30°, 60°, and 90° and for $\phi=0°$, 30°, 60°, and 90°, where ϕ is the angle between the molecular axis and the [100] direction (Fig. 5). At such a large distance from the surface the energetically most favorable entrance channel is over the fcc site, followed by hcp, bridge, and top sites. This is in agreement with results from LDA calculations.[4]

In order to examine the minimum-energy path, we calculate the O_2/Al(111) PES "by relaxation" for O_2 parallel to the surface ($\theta=90°$). Relaxation here means that the PES is calculated in a sequence of configurations $\mathbf{R}_i$ and from it the forces $\mathbf{f}_i$ on each atom are calculated. The atoms are propagated by action of these forces for a short time ($\approx$1 fs) to a new configuration $\mathbf{R}_{i+1}$. Then the PES is calculated for this new configuration $\mathbf{R}_{i+1}$, etc. We start at $Z=3.5$ Å, and in eight laterally different configurations, with the CM of the oxygen molecule over top, fcc, bridge, and hcp sites, respectively, using two in-plane molecular orientations ($\phi=0°$, 90°), as shown in Fig. 6. For the relaxation of the atomic position a DMD method is used. The coordinates of the whole system are relaxed using the DMD method, except for the Al atoms in the two innermost layers. In all cases, independently of the initial configuration (O_2 starting from 3.5 Å above the surface), the minimum of the energy is found, when the oxygen molecule is dissociated and the two O atoms are positioned at two neighboring fcc sites, at $Z\approx0.8$ Å above the Al surface layer.

The results also show that in all cases except one (the "gray channel") there is an open channel for the oxygen molecule to dissociate without any activation barrier, when $\theta=90°$. When O_2 is placed above the bridge site with $\phi=90°$ ("gray circles" in Fig. 6), the reaction path of adiabatic approach of O_2 to the surface shows an activation barrier of $E_b\approx0.2$ eV at $Z=2.3$ Å. This is in agreement with an independent calculation.[6]

To account for the rotational degrees of freedom of the oxygen molecule and also to get a deeper understanding of the dissociation process, a more extensive mapping of the three-dimensional PES are calculated for the molecule over the fcc, hcp, top, and bridge sites, with different orientations of the O_2 molecule relative to the surface normal. The PES cuts are displayed in Figs. 7–9 as level contours in a plane spanned by the intramolecular distance ($d_{O\text{-}O}$) and the molecular CM distance Z from Al surface.

Figure 7 shows the calculated PES of O_2 over the fcc hollow site, with $\phi=0°$ and $\theta=90°$, 60° 30°, 0°. All the cuts of the PES show that a barrier in the entrance channel is missing. This is in agreement with the limited mappings in previous theoretical works.[4–6] For a molecule with an inclination to the surface ($\theta\neq90°$) our calculation presents a new feature,[16] however. There is a molecularly chemisorbed state, a precursor to the dissociative chemisorption [cases of $\theta=60°$, 30°, and 0° above the fcc site in Fig. 7(b–d)]. The variation of the energy of the system along the reaction path is also plotted for all PES cuts. These inserted plots clearly show the energy well of the molecular state.

We also calculate the PES for the O_2 molecule above the hcp ($\phi=0°$ and $\theta=0°$, 90°; Fig. 8), top, and bridge sites (both at $\phi=0°$ and $\theta=90°$; Fig. 9). Even these cases lack activation barriers in the entrance channel but show a molecularly chemisorbed state for the molecule approaches with some inclination.

To experimentally observe an oxygen molecule trapped in this molecularly adsorbed state, quantities like chemisorption energy, bond length, charge, vibrational-stretch frequencies, and dissociation-energy barriers should be of interest. According to the PES, the molecular states ($\theta=0°$) are characterized by a molecular chemisorption energy in the range 1.5–2.1 eV, O-O bondlength 1.45–1.55 Å, vibrational-stretch frequency of 80–100 meV, and dissociation-energy barrier around 200–400 meV. To get vibrational-stretch frequency, the total energy of the system is calculated at the minimum with a small variation of the oxygen molecular bond length, a few percent of an angstrom, and then using

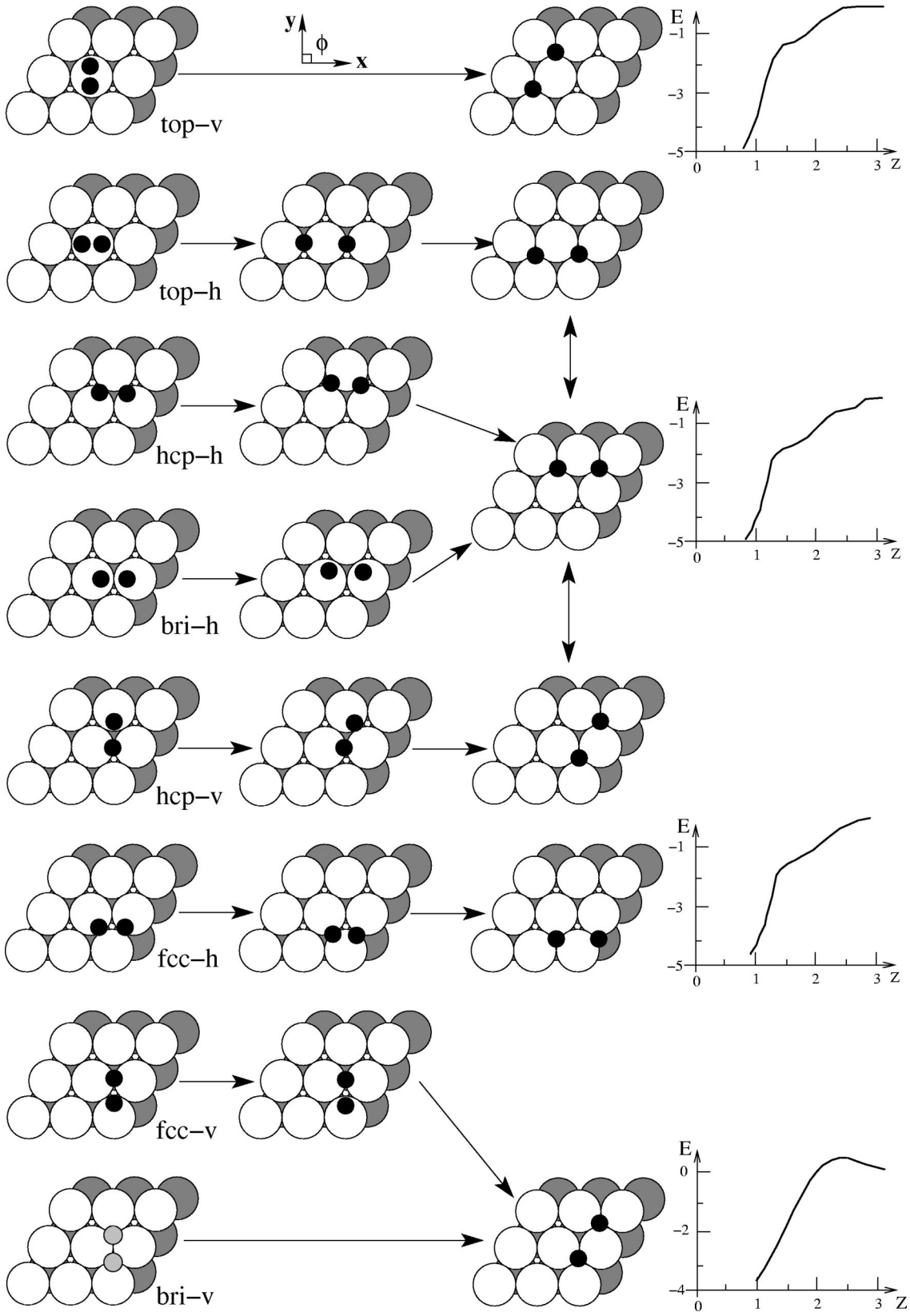

FIG. 6. Schematic figures for relaxation of an O_2 molecule with parallel orientation (θ=90°) in representative channels on the Al(111) surface (the small and large circles representing O and Al ions, respectively). The symbols *h* and *v* indicate ϕ=0° and 90°, respectively. Potential-energy curves (PEC) along the reaction path are also plotted for each configuration. The last channel (marked with small gray circles for the O_2 molecule) is the only one with an activation barrier.

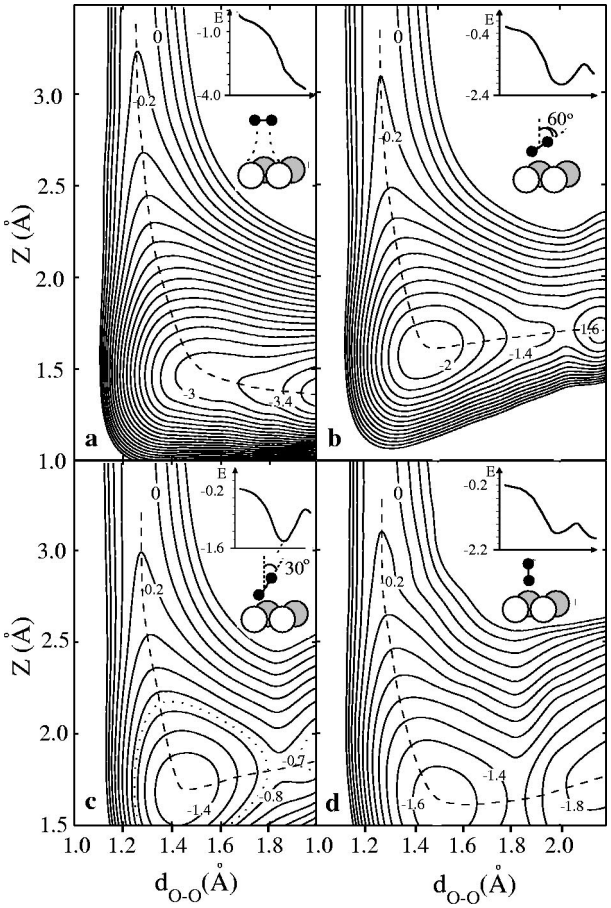

FIG. 7. Cuts through the six-dimensional PES of O_2 with bond length $d_{O\text{-}O}$, a distance Z above the Al(111) surface on fcc site. The molecule-surface angles θ are (a) 90°, (b) 60°, (c) 30°, and (d) 0°. The numbers in the equipotential contours are the energy values in eV measured from the energy of totally separated O_2 and Al(111) surface.

the harmonic approximation these frequencies were calculated. From explicit adsorbate-induced LDOS calculations, described in detail in the Discussion, the molecularly adsorbed state can be identified that for an $O_2{}^{2-}$ electron configuration.

In this paper just two-dimensional cuts through the sought six-dimensional PES are calculated. Although a complete mapping of the whole PES is needed to fully account for the molecular state, the arguments given in the following sections are general enough to warrant its existence. It is important to mention that the experimental results regarding the existence of such a molecular chemisorption state are contradictory.[3,15,17,23]

Section III C shows that the chemisorption of *atomic* oxygen involves quite some outward relaxation of the outermost Al layers. To understand the effects of surface relaxation in the stability of *molecular*-chemisorption state, oxygen molecules standing upright over hcp and fcc sites are considered. At several positions along the reaction path total-energy calculations are performed, where the three uppermost aluminum layers are allowed to relax using the DMD method.

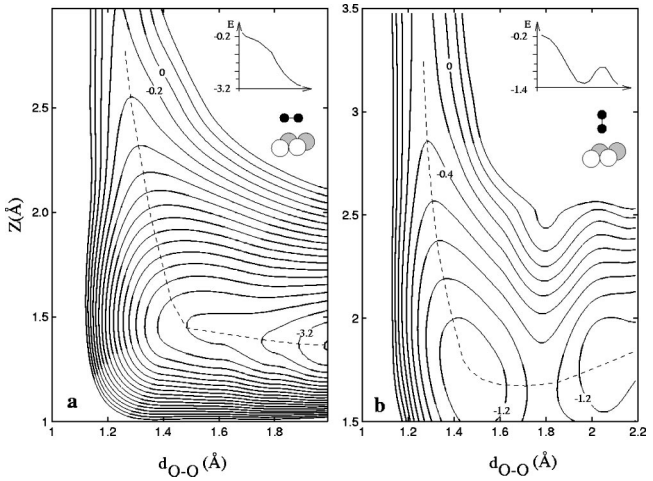

FIG. 8. Cuts through the six-dimensional PES of O_2 with bond length $d_{O\text{-}O}$, a distance Z above the Al(111) surface on hcp site. The molecule-surface angles θ are (a) 90° and (b) 0°. The numbers in the equipotential contours are the energy values in eV measured from the energy of totally separated O_2 and Al(111) surface.

The fcc result, Fig. 10, shows the presence of a stable molecularly chemisorbed state, with a barrier against dissociation of about 0.25 eV, almost identical to the value in the unrelaxed case. The outward interlayer relaxations are found sizable, approximately $\Delta d_{12} \approx +8.26\%$ and $\Delta d_{23} \approx +2.86\%$, respectively, compared to those of the clean aluminum surface. The reaction path is basically displaced by the same amount outwards. Similar result were also found for the molecular chemisorption state over the hcp site.

To answer the question of whether the molecular chemisorption state presented in Fig. 7(d) is a true local minimum, we performed multiple tests. The oxygen molecule was displaced slightly, both in z direction and along the surface, the bond length and the θ angle was changed in multiple ways,

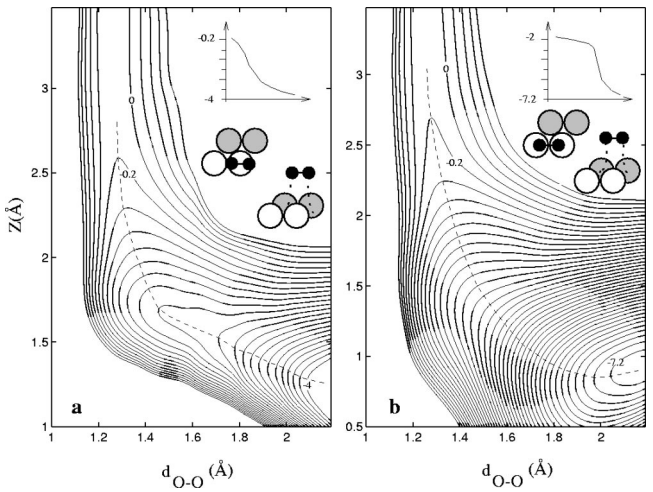

FIG. 9. Cuts through the six-dimensional PES of O_2 with bond length $d_{O\text{-}O}$, a distance Z above the Al(111) surface on (a) top site (ϕ=0° and θ=90°) and (b) bridge site (ϕ=0° and θ=90°). The numbers in the equipotential contours are the energy values in eV measured from the energy of totally separated O_2 and Al(111) surface. The insetted pictures show top and side views.

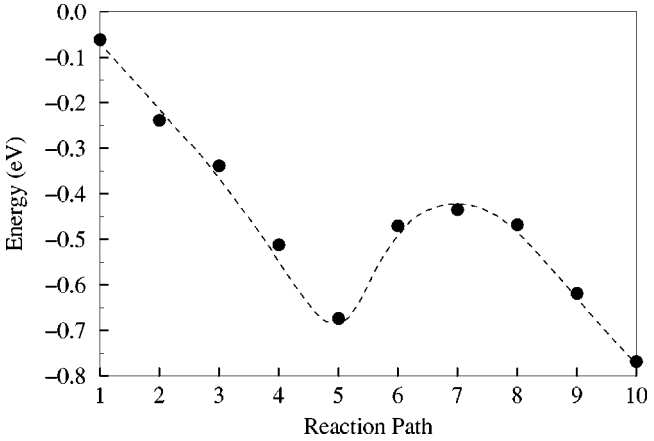

FIG. 10. Potential-energy curve along the reaction path with the O_2 molecule perpendicular on the fcc site (θ=0°), allowing the three uppermost Al layers to relax.

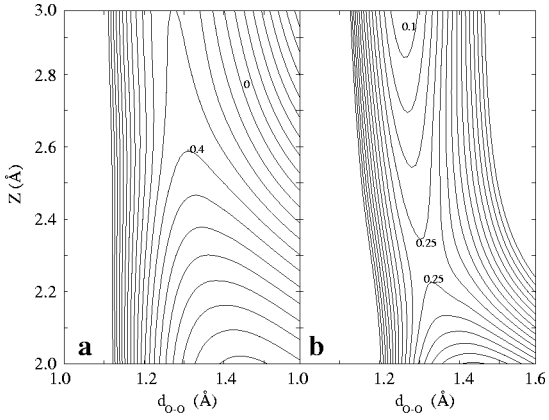

FIG. 11. Cuts through the six-dimensional PES of O_2 with bond length $d_{O\text{-}O}$, a distance Z above the Al(111) surface on (a) fcc site (θ=90°) and (b) bridge site (θ=90° and ϕ=0°) using the RPBE functional for the exchange-correlation functional.

then the whole system was relaxed. Regardless of the initial orientation and position of the O_2 molecule, the final structure relaxed to a position with $d_{O\text{-}O}$=1.45 Å, θ=0°, and Z =1.67 Å. Therefore we believe that this is a true local minimum. However, it is noticeable that a change of $d_{O\text{-}O}$ by more than 0.2 Å will push the molecule over the calculated barrier of 0.25 eV and start the dissociation process.

The calculations typically use the PW91 form of the GGA functional. The exchange-correlation energy-density functional has been found to be very sensitive to the strong density variations in the surface region.[29] It has also been speculated that such minute features as the activation-energy barrier in the ''gray channel'' of Fig. 6 could be an artifact of the GGA-PW91 functional and that the PBE,[32] revPBE,[33] and the RPBE (Ref. 29) functionals should give different and for the latter two cases more accurate results. The effects of these three new gradient-corrected functionals on the molecularly chemisorbed state (with the O_2 molecule perpendicular to the surface) are calculated in several positions along the reaction path. The result is that the molecularly chemisorbed state remains with almost the same depth as in PW91. Using the new functionals does not change our result about the absent activation barrier in the entrance channel either. This is seen by mapping parts of relevant cuts of the PES with the molecule far outside the surface and comparing the result with those calculated with PW91. The calculations are performed for two different configurations of the O_2 molecule parallel to the surface (θ=90°): (i) above the fcc site and (ii) above the bridge site with ϕ=90° as illustrated in Fig. 11. With the PW91 functional, the first one corresponds to the energetically most favored entrance channel, and the second one is the *only* entrance channel [gray channel of Fig. 6] that presents an activation barrier.

Figure 11 shows these calculated cuts of the PES to provide no entrance-channel activation barrier for the molecule on the fcc site (θ=90°) and an activation barrier with a size of 0.2 eV for the molecule on the bridge site (θ=90° and ϕ=90°). Hence, use of these new functionals does not change our previous results on an eventual activation barrier in the entrance channel.

F. Steering effect

In the preceding section some important features of the calculated adiabatic PES are highlighted, such as dissociation-energy barriers and molecular precursor states. The PES has also great importance for the dynamics, for instance, providing a steering effect. Such an effect makes impinging thermal and subthermal oxygen molecules approach the surface with a specific orientation, which should have great consequences for molecular trapping and abstraction.

To account for a possible steering effect in the entrance channel, we calculate total energies above the fcc site for θ=0°, 30°, 60°, and 90°, ϕ=0°, 30°, 60°, and 90°, and Z =3.0, 2.5, and 2.0 Å . The results in Table VII show the energy to vary with the angle ϕ and more importantly with the angle θ. This is interesting, as such a variation could be decisive for abstraction and molecular trapping.

Table VII shows the ϕ=30° orientation to be energetically favored for all considered angles θ and CM distances Z. The shown energy variation with respect to θ, with ϕ kept fixed at 30°, implies that the energetically most favored orientation is for θ=90° (parallel case). However, for the molecule to change its orientation from θ=0° to θ=90° there exists an energy barrier, with its maximum value at θ=30° for all the considered CM distances.

Of course, the steering effect requires a fully dynamic study. However, some indications can be obtained by just calculating the process on the individual atoms. The total-energy calculation allows Hellmann-Feynman forces to be obtained. Figure 12 gives some illustrations and an indication, whether they might rotate the molecule into some special orientation. Since the θ=30° and ϕ=30° orientation describes a local maximum in the calculated PES, for all the considered CM distances Z, the Hellmann-Feynmen forces on both oxygen atoms for this configuration have been calculated for CM distances Z=3.0, 2.5, and 2.0 Å, with $d_{O\text{-}O}$ kept fixed at 1.24 Å . To see in which direction these forces rotate the oxygen molecule, the effective torque τ for the molecule is also calculated. The result is τ=0.27, 0.31, and

TABLE VII. Total energies for the molecule with its CM above the fcc site, for CM distances $Z=3.0$ Å, 2.5 Å, and 2.0 Å, for $\theta=0°$, 30°, 60°, and 90°, and for $\phi=0°$, 30°, 60°, and 90°. The distance between the two O atoms is kept at the free-molecule value $d_{O\text{-}O}=1.24$ Å.

		θ			
		0°	30°	60°	90°
Z	3.0 Å				
$\phi=$	0°	−0.13	−0.11	−0.14	−0.17
	30°	−0.13	−0.13	−0.17	−0.17
	60°	−0.13	−0.11	−0.14	−0.16
	90°	−0.13	−0.09	−0.12	−0.16
Z	2.5 Å				
$\phi=$	0°	−0.27	−0.14	−0.15	−0.29
	30°	−0.27	−0.21	−0.25	−0.28
	60°	−0.27	−0.15	−0.15	−0.28
	90°	−0.27	−0.09	−0.05	−0.27
Z	2.0 Å				
$\phi=$	0°	−0.68	−0.45	−0.47	−0.70
	30°	−0.68	−0.57	−0.58	−0.70
	60°	−0.68	−0.46	−0.47	−0.69
	90°	−0.68	−0.35	−0.16	−0.69

0.43 eV for $Z=3.0$, 2.5, and 2.0 Å, respectively, where positive torque means a counterclockwise rotation.

Hence, according to this indication of the forces at play, oxygen molecules that approach the surface with an angle θ smaller than or equal to 30° would in this way end up with $\theta=0°$, i.e., perpendicular to the surface. Such molecules are apt for molecular adsorption and abstraction at dissociation. It is important to stress that the steering-effect considerations here are made only for the entrance channel above fcc sites. Entrance channels above other high-symmetry sites should exhibit a similar steering effect, however.

IV. DISCUSSION

The initial stage of aluminum oxidation, i.e., dissociation of the oxygen molecule on the aluminum surface, is not only an interesting topic but also a very difficult task. Understanding all mechanisms involved seems very hard but not impossible. From a theoretical point of view, $O_2/Al(111)$ is a molecule-surface system with a number of complicating additional features compared with a simple model system, e.g., H_2 on jellium. The adsorbate has more valence orbitals, both of σ and π type, and spin polarization is present already in the free molecule (Fig. 2). The substrate provides a structured surface and has a mix of *s*- and *p*-electron states as valence electrons. This versatility makes the $O_2/Al(111)$ system very interesting and educational to study. During the course of the present study, new experiments and more accurate theory have helped to deepen the understanding, leaving the confusion on a higher and more interesting level. This section provides discussions of an array of such mechanisms. It starts with some general comments and concludes with an attempt to assess the present situation.

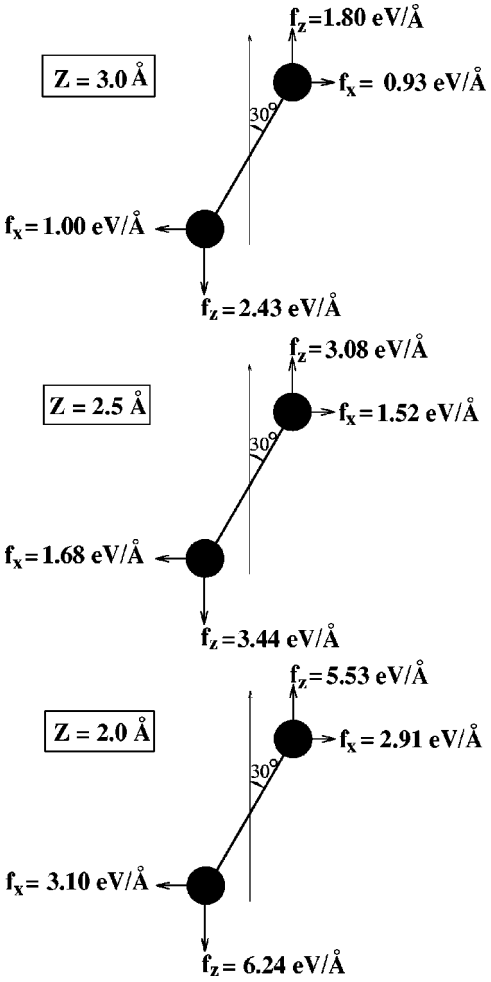

FIG. 12. The calculated Hellman-Feynman forces on each oxygen atom for three CM distances, $z=3.0$ Å, 2.5 Å, and 2.0 Å, and $d_{O\text{-}O}$ kept fixed at 1.24 Å.

In Sec. I, the present status of measured properties for the oxygen-aluminum system are reviewed. For several such properties, such as structure and energetics, chemisorption energy and site of atomically adsorbed oxygen (O_{ad}),[25] and diffusion-barrier energy and path of O_{ad},[25] agreement between theory and experiment has been achieved already before this study, which now confirms and refines the consistency. For other properties, such as the long-standing issue of wide separation of uncorrelated atomically adsorbed O atoms versus lacking correlation between atomically adsorbed O atoms after dissociation of O_2, there is a resolution provided by the present calculations[7,16] in combination with still more recent STM and resonantly enhanced multiphoton ionization experiments,[23,24] both revitalizing and establishing the abstraction view.[11] For another important issue, the low initial-sticking coefficient and its radical growth with increasing kinetic energy,[3] the present study adds to the confusion but might provide a platform for deepened studies. While it cannot provide an explanation for the sticking behavior, it sheds light on many interesting concepts, such as harpooning, mo-

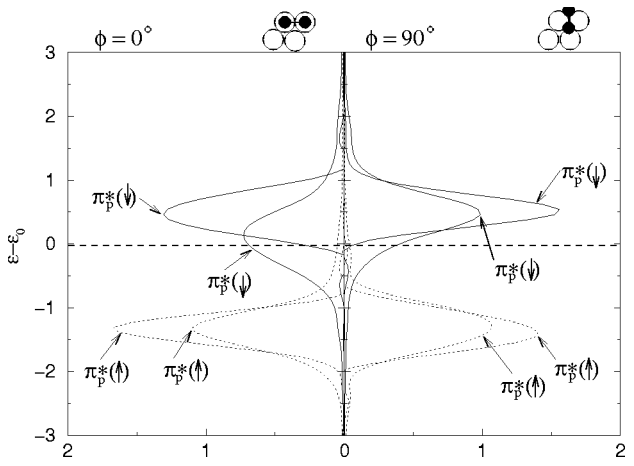

FIG. 13. Local density of states (LDOS) for the O_2 molecule at two orientations above the bridge site with (Z, $d_{O\text{-}O}$, ϕ) =(2.7, 1.24 Å, 0°) and (2.7, 1.24 Å, 90°). The spin-up and -down energy levels are explicitly indicated in the figure. The dashed line is the Fermi level.

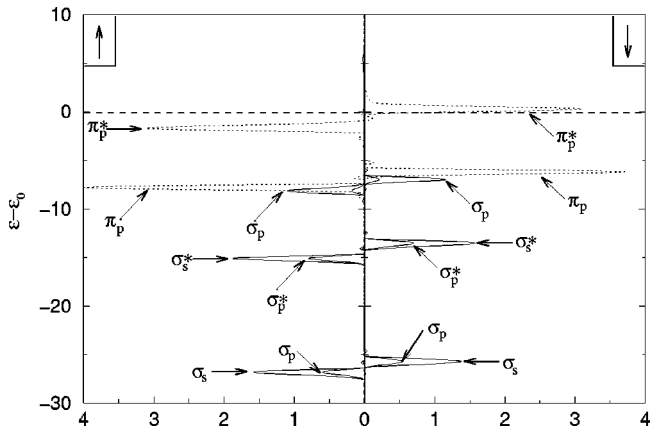

FIG. 14. Local density of states (LDOS) for the O_2 molecule above the fcc site with (Z, $d_{O\text{-}O}$, θ)=(3.0, 1.24 Å, 90°). The left and right panels show the spin-up and -down LDOS, respectively. The dashed line is the Fermi level.

lecularly chemisorbed state, spin-flipping, and abstraction. The identification of a molecularly chemisorbed state should have important implications for the dynamics and kinetics of oxygen adsorption.

A. Rare entrance-channel barriers

The measured thermal dissociative sticking probability, with its low initial value, $s_0 \approx 10^{-2}$, and its radical growth with impingement energy,[3] calls for a proper explanation. A simple-minded account for this behavior could have been promoted by the existence of an activation barrier in the entrance channel. However, as mentioned previously, all the considered entrance channels show no such barrier, except for one channel, when O_2 is placed above the bridge site with ϕ=90° (Figs. 6 and 11), referred to as the gray channel.

The latter barrier is linked to features already indicated in Fig. 6: The gray atoms lie in regions with no Al atoms directly underneath, i.e., with lower substrate-electron density and LDOS than in the other channels. This should give a smaller overlap between the molecule and substrate orbitals. This is confirmed by the calculated adsorbate-induced LDOS for an oxygen molecule at $Z=2.7$ Å outside the surface, 0.2 Å above the barrier, for two different entrance channels, namely, (i) the CM of the oxygen molecule over the bridge site with ϕ=90° (gray channel with the anomalous barrier) and (ii) the CM of the molecule over the same site with ϕ=0° (a channel with no energy barrier), shown in Fig. 13. The π_p^* lowest unoccupied molecular orbital with minority spin is seen to be shifted and filled less in the gray channel (ϕ=90°) than in the other channel (ϕ=0°). This results in a weaker bond to the surface. The kinetic-energy repulsion of O_2 then resides on a higher energy level. Further, crudely speaking, it is proportional to the substrate-electron density $n(\mathbf{r})$, and, with a slightly more refined argument, it relates to O_2 σ orbitals. Both arguments imply less corrugation than for the attraction, in particular, in view of surface smoothing.[59] At balance, this could result in an absolute energy barrier in the gray channel, as calculated. From this explanation of the existence of the barrier in the gray channel, we judge no other channel to have a similar activation barrier.

Hence, statistically, the gray channel is made significantly more rare by our calculations and considerations. In addition, the gray channel belongs to the energetically less-favored regions far outside the surface (The calculated total-energy values of O_2 with CM at 3.0 Å above the surface Al layer and with different molecular orientations over different sites show the channel over fcc site to be more favorale, followed by those over the hcp, bridge, and top sites).[7,16] Thus the barrier in the particular gray channel cannot explain the low value of the sticking coefficient for low incident kinetic energies.

B. Harpooning

In the asymptotic limit, i.e., when the molecule is far outside the surface, it senses a completely smooth surface. One question is how close to the surface does the PES continue to be smooth. In diabatic descriptions the PES kinetic-repulsion and adsorbate-substrate interference make it corrugated. The latter stretches relatively far out. Such an orbital-overlap effect as harpooning, i.e., the first transfer of an electronic charge from the surface to the antibonding orbital of the molecule, has been estimated to occur at 5–10 Å outside the surface for the prototype system Cl_2 on K.[13] Since the O_2 molecule has a much lower vertical electron affinity compared to Cl_2, and the Al(111) surface has a larger work function than the alkali metals, the charge transfer should occur much closer to the surface, i.e., in a region where the classical image picture should start to break down. This makes the O_2/Al(111) system more complicated than Cl_2/K. In the adiabatic picture the overlap required for such a tunneling gives interference effects, i.e., bonding effects. The LDOS calculated for the oxygen molecule at $Z=3.0$ Å illustrates this (Fig. 14).

Compared to the LDOS of the free molecule (Fig. 2) the changes are small. However, there is a slight shifting and

broadening of the molecular resonances. The orbital energies close to the Fermi level are particularly interesting, and there the $2p_{x,y}$-derived minority-spin π_p^* MO resonance, which is empty in the free molecule, is partially occupied already at $Z=3.0$ Å. This implies electron transfer to this orbital, with a concomitant reduction of the spin-magnetic moment. Due to its antibonding character, the intramolecular bond weakens. Beyond this, the changes of the LDOS, compared to that of the free molecule (Fig. 2) are small.

The observed overlap effects should be important for the early surface dynamics of impinging thermal molecules, in terms of, e.g., steering and channeling. It should be stressed, however, that the electrons in the adiabatic LDOS of Fig. 14 have infinite time to adjust to the presence of the surface.

C. Molecularly chemisorbed state

To analyze the molecular chemisorption state in more detail and understand the nature of this state, electronic structure is examined and several cuts of LDOS are calculated. The fcc site chosen for the analysis in this section is believed to be representative for all the sites.

The near-surface oxygen-induced LDOS distributions ($Z=1.3-1.8$ Å) above the fcc site in Fig. 15 show drastic changes, compared to the far-surface oxygen-induced LDOS in Fig. 14. They are calculated for representative $Z=1.4$ ($d_{\text{O-O}}=1.8$ Å and $\theta=0°$), $Z=1.7$ ($d_{\text{O-O}}=1.8$ Å and $\theta=30°$), $Z=1.7$ ($d_{\text{O-O}}=1.8$ Å and $\theta=60°$) and $Z=1.6$ ($d_{\text{O-O}}=1.8$ Å, and $\theta=90°$) orientations, as indicated in the figure, for the approach to the molecularly chemisorbed state.

The LDOS at the PES minimum shows the two $2p_{x,y}$-derived minority-spin π_p^* MOs to be shifted down below the Fermi level. As the σ_p^* orbital resonances still are unfilled, this means that the PES minimum corresponds to a molecular adsorbed state with an $O_2{}^{2-}$ electron configuration.

The spin-resolved LDOS curves in Fig. 15 for the dissociation barrier ($\theta\neq 90°$) and a similar O-O configuration parallel to the surface ($\theta=90°$) show the $2p_{x,y}$-derived minority-spin π_p^* MO resonance, empty in the free molecule and partially occupied in the parallel case ($\theta=90°$), to be pushed up and even above the Fermi level for $\theta=0°$. The mechanism behind this is indicated by, e.g., the sizable splitting of the σ_s levels, spin-up and -down, respectively. As shown in Fig. 16 this splitting is largest for $\theta=0°$ (about 8 eV) and decreases with decreasing angle. This is found to be due to an in-out shift, making the lower (upper) σ_s spin orbital reside on the inner (outer) O atom.[69] The shift is caused by the variation of the inner potential for the electrons in the surface region, which in the direction perpendicular to the Al surface is sizable.[69] Such a spatial and spin ''polarization'' also applies for the $2p_z$-derived O-O bonding σ_p spin-orbital resonance, where the inner one couples strongly to the Al atoms. ''Lacking'' other spin-majority orbitals on the outer atom, the π_p^* orbitals, located on this atom for $\theta\neq 90°$, benefit less from the exchange interaction and thus have a reduced shift from the free-molecule level, and thus less filling with electrons than for $\theta=90°$. Similarly the σ_p^* down-spin orbital is, in practice, empty there. The bond order in the $\theta\neq 90°$ cases is therefore relatively high, which is beneficial for the formation of a intramolecular bond. Thus one can conclude that a Hund's rule (maximal molecular spin for stability) effect is stabilizing the metastable molecularly chemisorbed state for O_2 with inequivalent atoms.

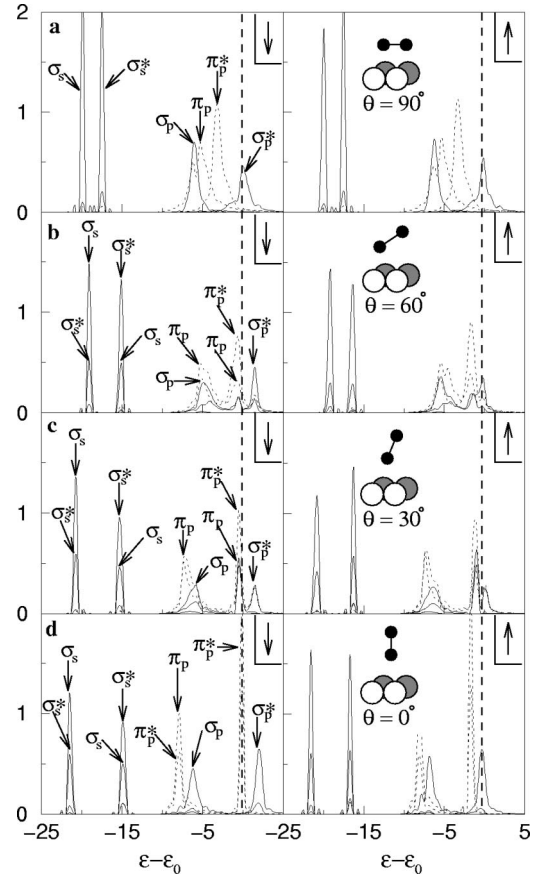

FIG. 15. Local density of states (LDOS) for the O_2 molecule above the fcc site with (a) (Z, $d_{\text{O-O}}$, θ) = (1.3, 1.8 Å, 90°), (b) (Z, $d_{\text{O-O}}$, θ)=(1.7, 1.8 Å, 60°), (c) (Z, $d_{\text{O-O}}$, θ)=(1.7, 1.8 Å, 30°), and (d) (Z, $d_{\text{O-O}}$, θ)=(1.6, 1.8 Å, 0°). The left and right panels show the spin-up and -down LDOS, respectively. The dashed line is the Fermi level.

For O_2 parallel to the surface, on the other hand, the constituting atoms are equivalent and this mechanism is missing. Thus the antibonding MO resonance has a more common variation with the distance to the surface, as illustrated in Fig. 15, and thus a more efficient filling. This could explain the absence of a molecular minimum in the upper left diagram of Figs. 8 and 9 and the diagrams of Fig. 10, i.e., the fact that the molecular configuration parallel to the surface behaves exceptionally.

Direct evidences for the temporary trapping in the predicted molecularly adsorbed state are still lacking. Indirect hints about a molecularly adsorbed state are given in the sticking study of Ref. 15 and in Refs. 70 and 71. However, more importantly, the very recent results of Ref. 23 are fully compatible with existence and properties of the molecular intermediate of our adiabatic PES.

The local minimum is shallow and the trapping probability remains to be calculated or measured. However, it lies in a region, ''the reaction zone'' (Z in the range from about 1 to

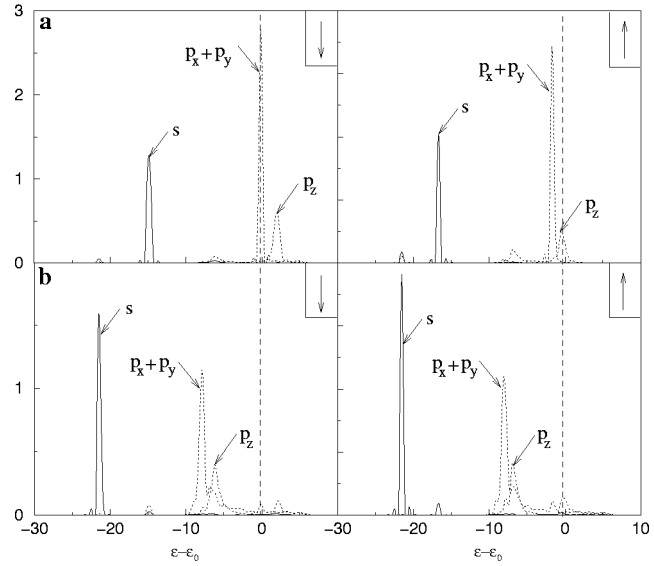

FIG. 16. Local density of states (LDOS) projected into atomic orbitals for (a) the outer oxygen atom and (b) the inner oxygen atom of an oxygen molecule at the fcc site with $Z=1.6$ Å and $d_{\text{O-O}}=1.8$ Å.

2 Å), where nonadiabatic processes, such as charge, spin, and energy transfers are very efficient. This is likely to make the molecules lose sufficient energy to make at least a few of them end up in the intermediate state. A fully dynamical description is certainly required, however. Some molecules are likely to run across the local shallow minimum and to dissociate into adsorbed O atoms in nearby fcc sites. It is interesting to note that our adiabatic PES thus supports the existence of correlated atomically adsorbed oxygen atoms in neighboring fcc sites, which has been observed in STM studies.[23,24]

D. Abstractive chemisorption

Chemisorption of molecules on metal surfaces can be associative, dissociative, or abstractive, i.e., as a whole molecule adsorbed on the surface, as one that dissociates into separate fragments on the surface, or as one that leaves only a part on the surface. Dissociative chemisorption can end directly into nearby sites or reach equilibrium first after a separation of some lattice constants, depending on, e.g., the corrugation of the surface. A contrast is found in the example of a diatomic molecule that hits the surface head on, i.e., with its axis more or less perpendicular to the surface, when one of the atoms can stick to the surface, while the other atom is repelled and ejected into the gas phase. Such a dissociation scenario is called abstractive chemisorption and has been reported for many systems,[11] e.g., halogens on the Si(111) surface.[19] Such a mechanism has also been proposed for the $O_2/\text{Al}(111)$ system.[13]

Our calculated adiabatic PES indicates that abstraction should occur for the $O_2/\text{Al}(111)$ system. This can be seen by looking at a PES cut for a nonparallel O_2 molecule ($\theta\neq 90°$), which does not only show the growing bond length $d_{\text{O-O}}$ of a molecule that gets over the dissociation barrier but

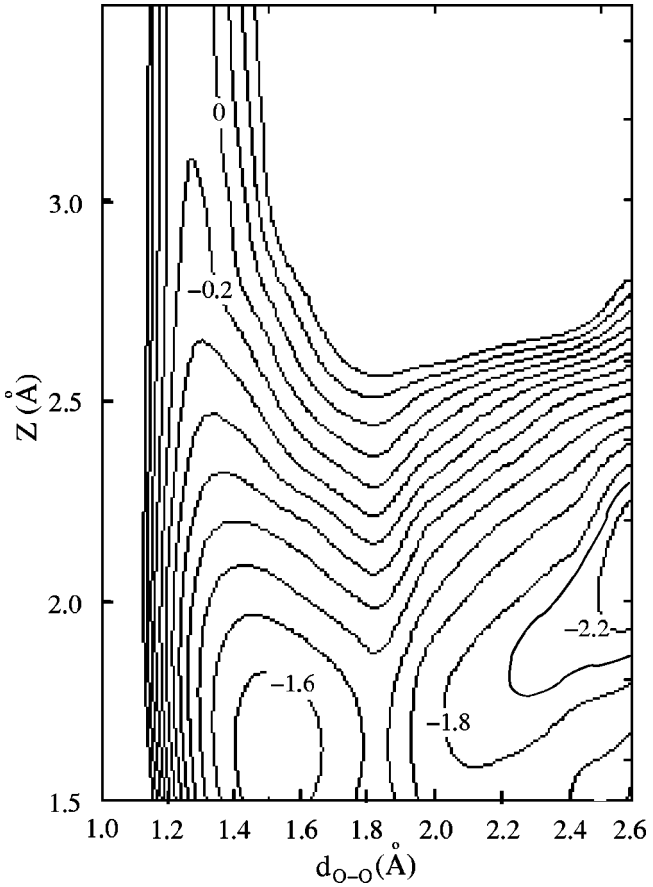

FIG. 17. The extended PES of O_2 molecule over fcc site with $\theta=0°$; for comparison see (d).

also a growing CM coordinate Z, ultimately beyond limits (computational reasons set a practical limit at $d_{\text{O-O}}=2.2$ Å, but the PES is expected to go downhill with increasing $d_{\text{O-O}}$). The $\theta\neq 90°$ orientation and the strong chemisorption of a single O atom implies that one O atom should stay on the surface and the other one leave, i.e., abstraction.[11,23] To demonstrate the pronounced limitation, we extended the PES for the O_2 molecule with $\theta=0°$. The CPU time needed for performing such extended calculations from 2.2 A to 2.6 Å was over 6 months, in terms of single CPU time. Furthermore the results, Fig. 17, confirm the proposed downhill trend of increasing $d_{\text{O-O}}$.

In order to have conditions for abstractive chemisorption, the oxygen molecule should hit the surface with its axis more or less perpendicular to it, so for impinging oxygen molecules, anisotropy really matters. Thermal molecules in a gas appear with equal weights on all orientations. A particular direction, such as parallel, thus has a small statistical weight. In the region close to the surface, however, there are steering effects that might favor some orientation. Two sources for alignment of impinging thermal and subthermal oxygen molecules into a perpendicular orientation are van der Waals and directional chemisorption forces, the latter expressed as a θ dependence of the PES. The van der Waals forces are weak but dominating for a molecule far outside the surface. The asymptotic form of the van der Waals energy in Sec. II D at, for instance, $Z=3.5$ Å is -42 and -49 meV for parallel and

perpendicular O_2, respectively. This slight anisotropy, which is comparable to thermal energies and energies calculated with GGA might steer impinging thermal and subthermal O_2 molecules to approach the surface in perpendicular orientations. The PES mapping and the total-energy results in Table VII show the energy, including that of the local minimum, to vary with angle θ. There is also an energy barrier for a molecule to change its orientation from $\theta=0°$ to $\theta=90°$ with its maximum value at about $\theta=30°$.

Furthermore, for oxygen molecules entering the zone, where nonadiabatic processes such as charge, spin, and energy transfers to substrate electrons, phonons, and magnons are very efficient [for O_2/Al(111) at Z values between 1 and 2 Å], some of them should lose sufficient energy to make at least a few of them temporarily trapped or thermalized in the intermediate molecular state on a cold Al(111) surface. Molecules entering with an angle θ smaller than about 30° would in this way end up with $\theta=0°$, i.e., perpendicular to the surface, and those with other angles would become parallel to it. The former ones are apt for precursor-molecule adsorption and for abstraction at dissociation. The dissociation out of this state is activated, and only one O atom should end up at the surface.

This abstraction channel is exothermic by about 2.8 eV, the bond energy of free O_2 being 5.11 eV and the chemisorption energy of O being 7.55 eV, according to experimental data. In the predicted abstraction the outer O atom is expected to end up as a neutral atom far outside the surface at adiabatic or near-adiabatic conditions. Inspection of the projected LDOS illustrated in [Fig. 15(d)] shows it to attain a $(2p)^4$ configuration already at $Z=1.6$ Å and $d_{O\text{-}O}=1.8$ Å, i.e., when the atom is 2.5 Å outside the surface layer.

As mentioned in the Introduction, the experimental studies in Ref. 23 clearly confirms our prediction about the existence of the abstraction channel in the O_2/Al(111) system. It also reports[23] on the simultaneous existence of uncorrelated atomically adsorbed oxygen atoms and correlated ones in neighboring fcc sites. Accordingly, at intermediate translational energies, a predominant fraction of the chemisorption events follow an abstraction mechanism, which provides a realistic explanation of the observation of the single chemisorbed oxygen atoms. The experimental observations of the abstraction channel and the existence of singles and pairs of oxygen atoms as end products are fully consistent with our theoretical study and have important ramifications.

It is important to stress that our study should be supplemented by a fully dynamical description to accurately estimate the importance of the abstraction mechanism for the dissociation of O_2 on the (111) surface of aluminum.

V. CONCLUSIONS AND OUTLOOK

In order to elucidate the fundamental processes governing the initial stage of aluminum oxidation, i.e., the dissociation of oxygen on an aluminum surface, a comprehensive DFT study of the multidimensional adiabatic potential-energy hypersurface (PES) is carried out. The exchange-correlation effects are accounted for by the generalized-gradient approximation (GGA).

The calculated cuts of the PES reveal a very complex system. A traditional activation barrier for dissociation is found to be very unlikely, occurring in only one of the many entrance channels. The dissociation process is shown to occur via an intermediate molecular-chemisorption precursor state with a low dissociation barrier. The molecular state is identified as having an "O^{2-}" electron configuration and is characterized by O-O bond lengths, vibrational-stretch frequencies, and dissociation-energy barriers in the ranges 1.45–1.55 Å, 80–100 meV, and 200–400 meV, respectively. The existence of the molecular state can be traced back to a Hund's rule spin effect that for the very inequivalent O atoms of the nonparallel O_2 close to the Al surface is stabilizing this state. An abstractive chemisorption mechanism is also predicted.

For the dynamics of O_2 on the Al(111) surface, these PES features should have important consequences. In order to obtain the molecule in the molecular chemisorption state, present for a nonparallel molecule, it has to dissipate quite a lot of energy. The oxygen molecule is very particular in this respect, having several dissipation channels. For each O_2 molecule, up to four electrons should be transferred before the dissociative chemisorption is completed. Nonadiabatic processes could be connected with such electron transfers, and energy could thereby be dissipated. In addition, the relative closeness of the O and Al atomic masses also makes phonon processes favorable. Finally, a spin-flip process should be able to generate spin waves (magnons). As the conditions for dissipation to electrons, magnons, and phonons are favorable, there should be a good chance for (temporarily) trapping some impinging thermal O_2 molecules in the molecularly adsorbed state on a cold Al(111) surface. The dissociation out of this state is activated, and only one O atom should end up on the surface. The other O atom is predicted to end up far outside the surface, i.e., abstraction of the atom. Arguments in favor of steering the molecule into a nonparallel orientation are given. The less likely parallel orientation should lead to O atoms adsorbed in neighboring fcc sites.

It should be stressed again that a fully dynamical description with dissipation is needed in order to account for the different mechanisms involved.

There have been early reports on molecularly adsorbed O_2 on Al(111).[15,70,71] Unfortunately, clear evidences that this is a property of the clean surface have been lacking. The very recent report[23] on measured single and paired O atoms and abstraction of O atoms is therefore very gratifying. The observed[3] very low initial thermal-dissociative-sticking probability, $s_0 \approx 10^{-2}$, and the radical growth of $s_0(E)$ with increasing impingement energy E remain to be explained, however, probably in terms of nonadiabatic processes.

The authors gratefully thank Igor Zoric and Bengt Kasemo for discussions and encouragement. The work was supported by the Natural Science Research Council and the Swedish Foundation for Strategic Research (SSF) via Materials Consortium No. 9, which is gratefully acknowledged. The work has benefitted from access to the UNICC supercomputers.

[1] N. Cabrera and N. F. Mott, Rep. Prog. Phys. **12**, 163 (1948-49).
[2] P. O. Gartland, Surf. Sci. **62**, 183 (1977).
[3] L. Österlund, I. Zoric, and B. Kasemo, Phys. Rev. B **55**, 15 452 (1997).
[4] J. Strömquist, Applied Physics Report No. 97, 1998 (unpublished).
[5] T. Sasaki and T. Ohono, Comput. Mater. Sci. **14**, 8 (1999).
[6] K. Honkala and K. Laasonen, Phys. Rev. Lett. **84**, 705 (2000).
[7] Y. Yourdshahyan, B. Razaznejad, and B. I. Lundqvist, Solid State Commun. **117**, 531 (2001).
[8] B. Kasemo, E. Törnquist, J. K. Nørskov, and B. I. Lundqvist, Surf. Sci. **89**, 554 (1979).
[9] B. Kasemo, Phys. Rev. Lett. **32**, 1114 (1974).
[10] J. K. Nørskov, D. M. Newns, and B. I. Lundqvist, Surf. Sci. **80**, 179 (1979).
[11] J. Strömquist, L. Hellberg, B. Kasemo, and B. I. Lundqvist, Surf. Sci. **352-354**, 435 (1996).
[12] M. Polanyi, *Atomic Reactions* (Williams and Norgate, London, 1932).
[13] L. Hellberg, J. Strömquist, B. Kasemo, and B. I. Lundqvist, Phys. Rev. Lett. **74**, 4742 (1995).
[14] K. Kato, T. Uda, and K. Terakura, Phys. Rev. Lett. **80**, 2000 (1998).
[15] V. Zhukov, I. Popova, and J. T. Yates, Jr., Surf. Sci. **441**, 251 (1999).
[16] Y. Yourdshahyan, Ph.D. thesis, Chalmers University of Technology and Göteborg University, Göteborg, Sweden, 1999.
[17] H. Brune, J. Wintterlin, R. J. Behm, and G. Ertl, Phys. Rev. Lett. **68**, 624 (1992).
[18] H. Brune, J. Wintterlin, J. Trost, G. Ertl, J. Wiechers, and R. J. Behm, J. Chem. Phys. **99**, 2128 (1993).
[19] J. Harris and B. Kasemo, Surf. Sci. **105**, L281 (1981).
[20] C. Engdahl and G. Wahnström, Surf. Sci. **312**, 429 (1994).
[21] G. Wahnström, A. B. Lee, and J. Strömquist, J. Chem. Phys. **105**, 326 (1996).
[22] J. A. Jensen, C. Yan, and A. C. Kummel, Science **267**, 493 (1995).
[23] M. Binetti, O. Weisse, E. Hasselbrink, A. J. Komrowski, and A. C. Kummel, Faraday Discuss. **117**, 313 (2000).
[24] M. Schmid (private communication).
[25] J. Jacobsen, B. Hammer, K. W. Jacobsen, and J. N. Nørskov, Phys. Rev. B **52**, 14 954 (1995).
[26] A. Kiejna and B. I. Lundqvist, Phys. Rev. B **63**, 085405 (2001).
[27] B. I. Lundqvist, A. Bogicevic, K. Carling, S. V. Dudiy, S. Gao, J. Hartford, P. Hyldgaard, N. Jacobson, D. C. Langreth, N. Lorente, S. Ovesson, B. Razaznejad, C. Ruberto, H. Rydberg, E. Schröder, S. I. Simak, G. Wahnström, and Y. Yourdshahyan, Surf. Sci. **493**, 253 (2001).
[28] W. Kohn and L. J. Sham, Phys. Rev. **140**, A1133 (1965); **145**, A561 (1966).
[29] B. Hammer, L. B. Hansen, and J. N. Nørskov, Phys. Rev. B **59**, 7413 (1999).
[30] J. P. Perdew *et al.*, Phys. Rev. B **46**, 6671 (1992).
[31] J. P. Perdew, in *Electronic Structure of Solids '91*, edited by P. Ziesche and H. Eschrig (Akademie Verlag, Berlin, 1991), p. 11.
[32] J. P. Perdew, K. Burke, and M. Ernhzerhof, Phys. Rev. Lett. **77**, 3865 (1996).
[33] Y. Zhang and W. Yang, Phys. Rev. Lett. **80**, 890 (1998).
[34] G. Kresse and J. Furthmüller, Comput. Mater. Sci. **6**, 15 (1996).
[35] D. Vanderbilt, Phys. Rev. B **41**, 7892 (1990).
[36] H. J. Monkhorst and J. D. Pack, Phys. Rev. B **13**, 5188 (1976).
[37] L. Bengtsoon, Phys. Rev. B **59**, 12 301 (1999).
[38] G. Mills, H. Jonsson, and G. K. Schenter, Surf. Sci. **324**, 305 (1995).
[39] I. H. Lee and R. M. Martin, Phys. Rev. B **56**, 7197 (1997).
[40] A. Khein, D. J. Singh, and C. J. Umrigar, Phys. Rev. B **51**, 4105 (1995).
[41] A. D. Corso, A. Pasquarello, A. Baldereschi, and R. Car, Phys. Rev. B **53**, 1180 (1993).
[42] C. Filippi, D. J. Singh, and C. J. Umrigar, Phys. Rev. B **50**, 14 947 (1994); A. Khein, D. J. Singh, and C. J. Umringar, *ibid.* **51**, 4105 (1995).
[43] Y. S. Touloukian, *Thermophysical Properties of Matter* (Plenum, New York, 1975), Vol. 12.
[44] G. Simmons and H. Wang, *Single Crystal Elastic Constants and Calculated Aggregate Properties: A Handbook*, 2nd ed. (MIT Press, Cambridge, MA, 1971).
[45] G. N. Kamm and G. A. Alers, J. Appl. Phys. **35**, 327 (1964).
[46] J. Vallin, M. Mongy, K. Salama, and O. Beckman, J. Appl. Phys. **35**, 1825 (1964).
[47] C. Kittel, *Introduction to Solid State Physics*, 6th ed. (Wiley, New York, 1989).
[48] J. C. Boettger, Phys. Rev. B **53**, 13 133 (1996).
[49] P. J. Feibelman, Phys. Rev. B **46**, 15 416 (1992).
[50] J. Furthmüller, G. Kresse, J. Hafner, R. Stumpf, and M. Scheffler, Phys. Rev. Lett. **74**, 5084 (1995).
[51] U. Landman, R. Hill, and M. Mostoller, Phys. Rev. B **21**, 448 (1980).
[52] J. Schöchlin, K. P. Bohnen, and K. M. Ho, Surf. Sci. **324**, 113 (1995).
[53] J. R. Noonan and H. L. Davis, J. Vac. Sci. Technol. A **83**, 2671 (1990).
[54] H. B. Nielsen and D. L. Adams, J. Phys. C **15**, 615 (1982).
[55] J. K. Grepstad, P. O. Gartland, and B. J. Slagsvold, Surf. Sci. **57**, 348 (1976).
[56] D. Sigel (private communication).
[57] W. R. Tyson and W. A. Miller, Surf. Sci. **62**, 267 (1977).
[58] C. J. Fall, N. Binggeli, and A. Baldereschi, Phys. Rev. B **58**, 7544 (1998).
[59] R. Smoluchowski, Phys. Rev. **60**, 661 (1941).
[60] J. Trost, H. Brune, J. Wintterlin, R. J. Behm, and G. Ertl, J. Chem. Phys. **108**, 1740 (1998).
[61] A. Bogicevic, Johan Strömquist, and Bengt I. Lundquist, and Phys. Rev. B **57**, R4289 (1998).
[62] J. D. Head, Surf. Sci. **384**, 224 (1997).
[63] E. Zaremba and W. Kohn, Phys. Rev. B **13**, 2270 (1976).
[64] E. Hult, H. Rydberg, B. I. Lundqvist, and D. C. Langreth, Phys. Rev. B **59**, 4708 (1999).
[65] J. Harris and P. J. Feibelman, Surf. Sci. **83**, L133 (1982).
[66] B. I. Lundqvist, Y. Andersson, H. Shao, S. Chan, and D. C. Langreth, Int. J. Quantum Chem. **56**, 247 (1995).
[67] E. Hult, Y. Andersson, B. I. Lundqvist, and D. C. Langreth, Phys. Rev. Lett. **77**, 2029 (1996).
[68] E. Hult and H. Rydberg (private communication).
[69] H. Hjelmberg, B. I. Lundqvist, and J. K. Nørskov, Phys. Scr. **20**, 192 (1979).
[70] P. Hofman, K. Horn, and A. M. Bradshaw, Surf. Sci. Lett. **82**, 610 (1979).
[71] C. Astaldi, P. Geng, and K. Jacobi, J. Electron Spectrosc. Relat. Phenom. **44**, 175 (1987).